

Article

# In vivo proton MR spectroscopic imaging of colon cancer for non-invasive assessment of 5-FU resistance: A preliminary study

Qi Xie<sup>1,\*†</sup>, Xi-Yan Shao<sup>2,†</sup>, Yi-Ming Yang<sup>3,†</sup>, Min-Yi Wu<sup>4</sup>, Jing Zhang<sup>5</sup><sup>1</sup> Medical Imaging Department of Nansha, Guangzhou First People's Hospital, School of Medicine, South China University of Technology, Guangzhou 511457, China<sup>2</sup> Department of Ultrasound Medicine, The Second Affiliated Hospital, School of Medicine, The Chinese University of Hong Kong (Shenzhen), Shenzhen 518172, China<sup>3</sup> Department of Radiology, The Second Affiliated Hospital of Guangzhou University of Chinese Medicine, Guangdong Provincial Hospital of Traditional Chinese Medicine, Guangzhou 510006, China<sup>4</sup> Department of Radiology, Panyu Central Hospital of Guangzhou, Guangzhou 440113, China<sup>5</sup> Pathology Department, Cancer Center, Sun Yat-sen University, Guangzhou 510080, China\* **Corresponding author:** Qi Xie, [xieqi8@yeah.net](mailto:xieqi8@yeah.net), [eyqixie@scut.edu.cn](mailto:eyqixie@scut.edu.cn)

† These authors are co-first authors and contributed equally to this work.

## CITATION

Xie Q, Shao XY, Yang YM, et al. In vivo proton MR spectroscopic imaging of colon cancer for non-invasive assessment of 5-FU resistance: A preliminary study. *Imaging and Radiation Research*. 2025; 8(1): 11605. <https://doi.org/10.24294/irr11605>

## ARTICLE INFO

Received: 17 March 2025

Accepted: 27 May 2025

Available online: 27 June 2025

## COPYRIGHT



Copyright © 2025 by author(s). *Imaging and Radiation Research* is published by EnPress Publisher, LLC. This work is licensed under the Creative Commons Attribution (CC BY) license. <https://creativecommons.org/licenses/by/4.0/>

**Abstract:** Instant and accurate evaluation of drug resistance in tumors before and during chemotherapy is important for patients with advanced colon cancer and is beneficial for prolonging their progression-free survival time. Here, the possible biomarkers that reflect the drug resistance of colon cancer were investigated using proton magnetic resonance spectroscopy (1H-MRS) in vivo. SW480[5-fluorouracil(5-FU)-responsive] and SW480/5-FU (5-FU-resistant) xenograft models were generated and subjected to in vivo 1H-MRS examinations when the maximum tumor diameter reached 1–1.5 cm. The areas under the peaks for metabolites, including choline (Cho), lactate (Lac), glutamine/glutamate (Glx), and myo-inositol (Ins)/creatine (Cr) in the tumors, were analyzed between two groups. The resistance-related protein expression, cell morphology, necrosis, apoptosis, and cell survival of these tumor specimens were assessed. The content for tCho, Lac, Glx, and Ins/Cr in the tumors of the SW480 group was significantly lower than that of the SW480/5-FU group ( $P < 0.05$ ). While there was no significant difference in the degree of necrosis and apoptosis rate of tumor cells between the two groups ( $P > 0.05$ ), the tumor cells of the SW480/5-FU showed a higher cell density and larger nuclei. The expression levels of resistance-related proteins (P-gp, MPR1, PKC) in the SW480 group were lower than those in the SW480/5-FU group ( $P < 0.01$ ). The survival rate of 5-FU-resistant colon cancer cells was significantly higher than that of 5-FU-responsive ones at 5-FU concentrations greater than 2.5  $\mu\text{g/mL}$  ( $P < 0.05$ ). These results suggest that alterations in tCho, Lac, Glx1, Glx2, and Ins/Cr detected by 1H-MRS may be used for monitoring tumor resistance to 5-FU in vivo.

**Keywords:** 1H-MRS; MRI; human colon cancer; xenograft; nude mice; 5-FU resistance

## 1. Introduction

Patients with advanced colorectal cancer (CRC) mainly receive 5-fluorouracil (5-FU)-based palliative chemotherapy. For these patients, resistance to chemotherapeutic agents is the main reason for poor treatment effects [1]. Thus, resensitizing CRC cells to 5-FU-based chemotherapy is one of the important ways to overcome this obstacle. Instant and accurate evaluation of drug resistance in tumor tissues before and during chemotherapy is important for patients with advanced colon cancer.

At present, the detection of drug resistance in tumors involves in vitro drug

susceptibility experiments from the cellular level to the genetic level [2,3]. These methods can only detect the drug resistance of tumor tissues by invasively obtaining tumor specimens. Cellular metabolism is a sophisticated process that is heavily influenced by the surrounding microenvironment [4]. In vitro susceptibility tests may result in metabolite alterations in the removed tumor tissue, which may ultimately affect the results of the experiment. Therefore, it is necessary to explore new methods for promptly and precisely monitoring tumor drug sensitivity in vivo.

Proton magnetic resonance spectroscopy (1H-MRS) is a non-invasive imaging technique that measures the level of proton-containing compounds in tissues to explore biochemical metabolism information [5,6]. MRS does not involve a specific and sophisticated sample preparation process and indirectly provides information on transformations in tissue and organ metabolism by detecting dynamic changes in metabolite levels in a non-invasive manner in vivo [7].

As a non-invasive imaging technology, 1H-MRS has been widely used in the clinical evaluation of brain tumors [8,9]. 1H-MRS is helpful for the differential diagnosis, histological grading, and evaluation of the degree of infiltration in brain tumors [9]. 1H-MRS is also used for the assessment of tumor recurrence and therapeutic effects when there are difficulties in differentiating radiation necrosis from tumors with conventional MR imaging [8,9].

Chemotherapy-resistant cancer cells are able to survive in a hostile microenvironment with chemotherapeutic drugs. The potential metabolic characteristics that can reflect the drug resistance of cancer cells need further study. However, 1H-MRS has rarely been applied in the evaluation of tumor drug resistance.

Based on our previous studies [10–12], we hypothesize that 1H-MRS can detect changes in certain metabolites before and after the development of tumor drug resistance and may be a new way to detect molecular markers of tumor resistance evolution in vivo.

In this study, a 3.0-T clinical medical MRI system and matched animal coils were used to examine 5-FU-responsive and 5-FU-resistant human colon cancer tissues from preclinical models using 1H-MRS technology. We aimed to analyze the metabolic characteristics of 5-FU-responsive and 5-FU-resistant human colon cancer tissues via 1H-MRS and explore possible characteristic metabolites (imaging biomarkers) of tumor drug resistance.

## **2. Materials and methods**

All experiments were performed according to protocols approved by the Ethical Committee of Guangzhou Medical University for Animal Research and complied with the Guide for the Care and Use of Laboratory Animals (GY2017-007) [10–13].

### **2.1. Construction of a resistant human colon cancer cell line**

The parental human colon cancer cell line (SW480) used in this experiment was from the same research institution previously studied by our research group [10–13].

SW480 cell screening was similar to our previous research, using high-dose 5-FU (Xudong Haipu Pharmaceutical Co., Ltd., Shanghai, China) shock assay [11,13]. The SW480 parental cell line was cultured in RPMI 1640 medium containing 10%

fetal bovine serum (Gibco, Invitrogen, Waltham, MA, United States) and 100 units/mL penicillin (Solarbio Life Science, Beijing, China). A CO<sub>2</sub> incubator was used to incubate the cells at 37 °C with 5% CO<sub>2</sub> and saturated humidity. During the logarithmic growth phase, the SW480 cell was washed with BPS and incubated in medium with 6 µg/mL 5-FU for 24 h, followed by RPMI 1640 medium. The RPMI 1640 medium was replaced every 48 h. When the cells returned to their normal growth state, the same concentration of 5-FU was added for 24 h again. After 6 months of continuous drug screening by repeating the aforementioned steps, a 5-FU-resistant cancer cell line capable of stable growth at a concentration of 6 µg/mL 5-FU was obtained, and the cell line was designated SW480/5-FU.

The relative cell viability of SW480 and SW480/5-FU cells was measured by 3-(4,5-dimethyl-2-thiazolyl)-2,5-diphenyl-2-H-tetrazolium bromide (MTT) assay. Cells (SW480 or SW480/5-FU) in the logarithmic growth phase were incubated in 96-well plates (approximately 3000 per well). Seven groups treated with 5-FU (0.5, 1.25, 2.5, 5, 10, 50, 250 µg/mL) and a control group were set up with five duplicate wells per group. Ten microliters of MTT was added. The absorbance was collected by a multifunction microplate reader (American Berten Instrument Co., Ltd., Vermont, USA) at 490 nm.

The half-maximal inhibitory concentration (IC<sub>50</sub>) of 5-FU in SW480 and SW480/5-FU cells was acquired using SPSS v13.0 statistical software (IBM, Chicago, USA) [11,13]. The resistance index (RI) of SW480/5-FU cells was calculated as follows [11,13]: IC<sub>50</sub> of SW480/5-FU cells/IC<sub>50</sub> of SW480 cells = 20.594 µg/mL/4.639 µg/mL = 4.44.

## **2.2. SW480 and SW480/5-FU tumor xenograft models in nude mice**

BALB/c nude mice were purchased from the same research institution (No. 44007200046136) as in previous studies [11,13].

10 healthy BALB/c nude mice (female, 5–6 weeks, 16–18 g) were split into two groups: SW480/5-FU (5 mice) and SW480 (5 mice) randomly. SW480 (responsive group) or SW480/5-FU (resistant group) cell suspensions (0.2 mL, cell concentration  $4 \times 10^7$ /mL) were injected subcutaneously into the bilateral hind leg roots of nude mice. All mice were cultured in the specific-pathogen-free (SPF) laboratory of the Animal Experimental Center of Guangzhou Medical University (Guangzhou, China).

The maximum diameter of mouse tumors is limited to less than 1.5 cm according to the ethical standard of mouse tumor burden in the “2010 guidelines for animal welfare and use in cancer research” [11,14]. MRI examined tumors with a maximum diameter of 1–1.48 cm (mean 1.31 cm).

## **2.3. In Vivo MRI/MRS**

The tumor-bearing mice were subjected to MRI under warm conditions and anesthesia with intraperitoneal injection of 1 mL/100 g weight of 4% chloral hydrate (Qilu Hospital of Shandong University, Shandong, China) as previously described [10].

The MRI system included a 3.0-T clinical scanner (Magnetom Skyra, Siemens Healthcare, Erlangen, Germany) equipped with an XQ gradient system (maximum

gradient strength of 45 mT/m with a slew rate of 200 T/m/s) and an 8-channel mouse coil for signal reception (Chenguang Medical Technology Co., Shanghai, China). Sequences included morphological T2-weighted (T2W) fast spin-echo (TSE) images used for positioning-spectroscopic volume of interest (VOI) and 1H-MRS.

For T2W (TSE) imaging, the main scan parameters were as follows: repetition time (TR)/echo time (TE) = 4500 ms/110 ms, slice thickness = 2 mm, interval = 0, field of view (FOV) = 128 mm, number of signal averages (NSA) = 4, SENSitivity Encoding (SENSE) value = 2, acquisition matrix = 128 × 128, reconstruction matrix = 512 × 512, axial, coronal, sagittal imaging. Acquisition time = 2 min 2 s.

For 1H-MRS, multivoxel three-dimensional volume (3DMV) acquisition was performed using a Mescher-Garwood point-resolved spectroscopy sequence (MEGA-PRESS) covering the whole mass. The six outer volume saturation bands were manually applied at the edges of the VOI to minimize contamination from adjacent structures. Manual water suppression and shimming were performed until the value of the full width at half maximum (FWHM) was less than 40 Hz. Main scan parameters were as follows: spectral line bandwidth = 1000 Hz, flip angle = 90°, TR = 1700 ms, TE = 40 ms, slice thickness = 2 mm, slice gap = 0, FOV = 60 mm, VOI = 30 mm, acquisition voxel size = 4–9 mm, number of excitations (NEX) = 8, collection matrix = 128 × 128, Rel SNR = 1. Scan time = 9 min 13 s.

The spectral raw data (IMA file) was post-processed with software from the manufacturer (syngo MR D13, Siemens) by two radiologists (Yang YM, Wu MY), who were blinded to tumor grouping. Semiquantitative spectroscopic analysis of tumors (the area under the peak) was performed automatically in the integral of metabolites as previously described, avoiding necrotic areas or minimizing the necrotic areas on T2WI images [11]. The average value was divided by the volume of the voxel for normalization for statistical analysis to eliminate the potential influence of selection bias. Post-processing steps for the data included water reference processing, data filtering with the Hanning filter, zero-filling of the data, Fourier transformation, frequency shift correction, automatic baseline and phase correction, and curve fitting of the signal peak using the Gaussian line shape. The analyzed metabolites included creatine (Cr, 3.02 ppm), choline-containing compounds (tCho, 3.23 ppm), lactate (Lac, 1.31 ppm), myo-inositol (Ins, 3.56 ppm), and the glutamate and glutamine complex (two main peaks that are in relation to the Glu and Gln complex, Glx1 peak: 2.1–2.4 ppm, Glx2 peak: 3.65–3.8 ppm). tCho/Cr, Lac/Cr, Ins/Cr, and Glx/Cr values were obtained by automatic calculation for each voxel of tumor.

#### **2.4. Experimental study of tumor tissue**

After MR examination, 1–2 mL of 4% chloral hydrate was administered to the tumor-bearing mice by intraperitoneal injection. Then, the tumors were removed and divided into three parts for further study. Protein expression was detected using Western blotting; the assessed proteins included protein kinase C (PKC), permeability glycoprotein (P-gp, MDR), and multidrug resistance-associated protein 1 (MRP1). Histopathological examination and TUNEL and MTT assays were also conducted.

The Western blot detection of tumor resistance-related proteins was entrusted to Guangzhou Jetway Biotech Co., Ltd. in strict accordance with the operating manual

(Phototope<sup>®</sup>-HRP Western Blot Kit, Cell Signaling Technology, Danvers, USA). The antibodies included goat anti-mouse IgG/HRP (Abclonal, Wuhan, China), MDR1 (Abclonal, Wuhan, China), MRP1 (Abclonal, Wuhan, China), and PKC (Abclonal, Wuhan, China). The bands of the abovementioned proteins were scanned into JPG-format image files for further analysis. The integral optical density (IOD) of the bands was automatically assessed with Image-Pro Plus 6.0 software (Media Cybernetics Inc., San Diego, USA). The relative IOD (RIOD) of the abovementioned proteins was calculated by dividing the IOD of the target protein by the IOD of the internal reference (GAPDH).

Tumor histomorphology was assessed on hematoxylin and eosin (HE)-stained sections. Pathological sections were stained using the TUNEL apoptosis in situ detection reagent kit (Keygen, Jiangsu, China) according to the manufacturer's instructions as previously described [10].

The pathological slices were assessed by a pathologist (Jing Zhang) with over 20 years of professional experience.

Tumor necrosis was evaluated on tumor HE-stained slices at 400 $\times$  magnification, and the degree of necrosis was rated as 0–5 (points) by the pathologist as previously described [11], according to the necrotic area occupied in tumor tissues. The tumor cell apoptosis rate was calculated as the percentage of positively stained nuclei (dark brown) at 400 $\times$  magnification [12]. An in vitro susceptibility test was performed to detect the 5-FU resistance of human colon cancer xenografts according to a standard procedure as previously described [10]. The IC<sub>50</sub> values of the SW480/5-FU group and SW480 group were measured by MTT assay.

## 2.5. Statistical analysis

Statistical analysis was conducted using the SPSS statistical software package (version 25, IBM, Chicago, USA). The analysis indicator values were expressed as mean  $\pm$  standard deviation (SD). The Kolmogorov-Smirnov test was used for the normal distribution test. Due to the normal distribution ( $P > 0.05$ ), a paired *t*-test was used to compare Lac and Glx (Glx1, Glx2) between the SW480 group and the SW480/5-FU group. The other observed indicators of the two groups did not follow a normal distribution, and the Mann-Whitney *U* test was used for comparative analysis. The Spearman correlation test was used to analyze the correlation between metabolites and the expression of tumor resistance-related proteins. The difference was statistically significant when  $P < 0.05$ .

## 3. Results

Eight tumors in each of the SW480 and SW480/5-FU groups with maximum diameters near 1.5 cm were included in the study.

### 3.1. Metabolic profiles of SW480 and SW480/5-FU tumor tissues

The peaks of Cr, tCho, Lac, Ins, and Glx (Glx1, Glx2) were identified in the <sup>1</sup>H NMR spectra of SW480 and SW480/5-FU tumor tissues. **Figures 1–5** show stack plots of the corresponding metabolite images of SW480 (A) and SW480/5-FU (B)-derived tumor tissues. The metabolite images of tCho, Lac, Glx1, Glx2 and Ins/Cr show that

the corresponding metabolites are increased in the SW480/5-FU group, with higher signals than the SW480 group.

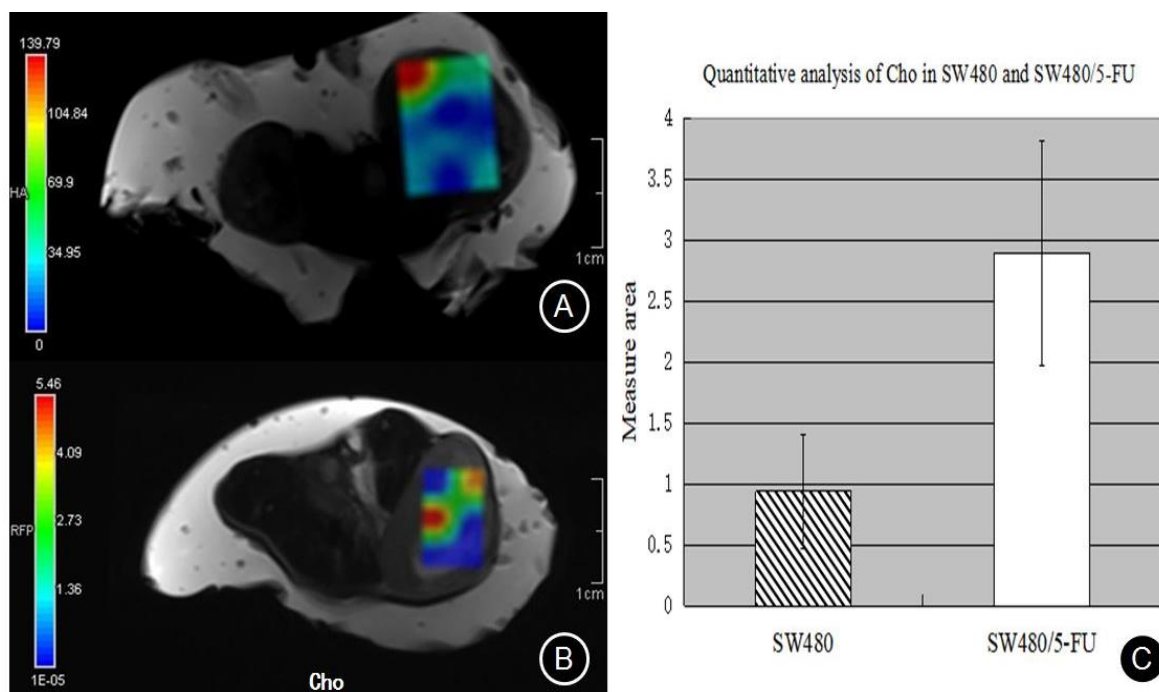


**Figure 1.** Metabolite image of the Cho profile in (A) SW480; (B) SW480/5-FU tumor tissues; (C) the area under the peak.

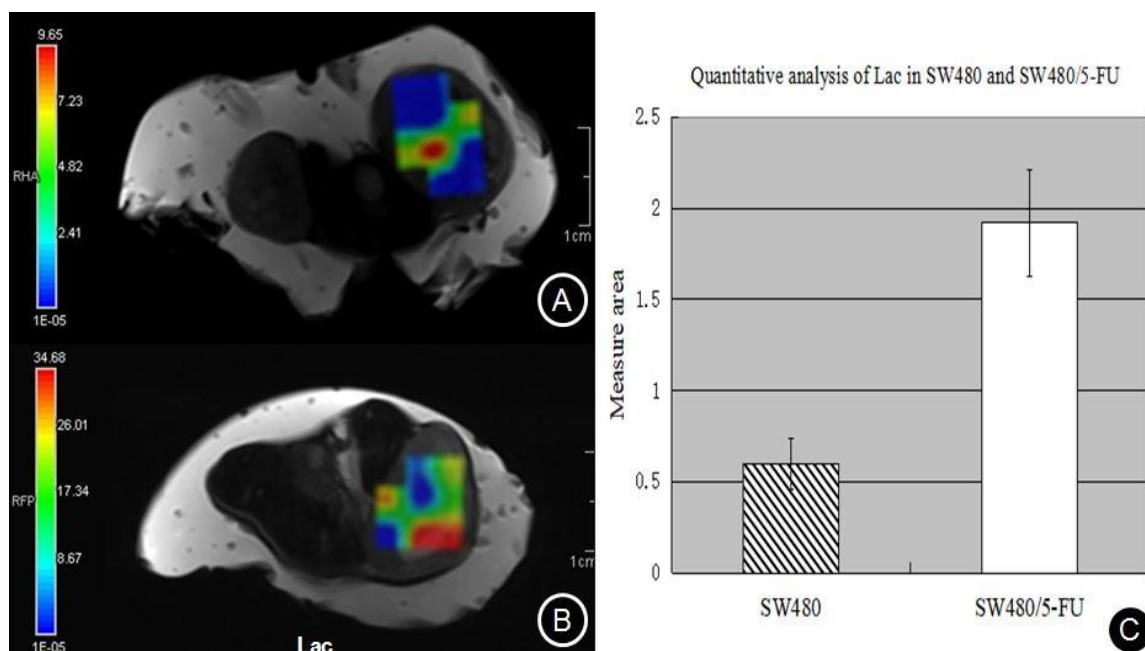


**Figure 2.** Metabolite image of the Lac profile in (A) SW480; (B) SW480/5-FU tumor tissues; (C) the area under the peak.

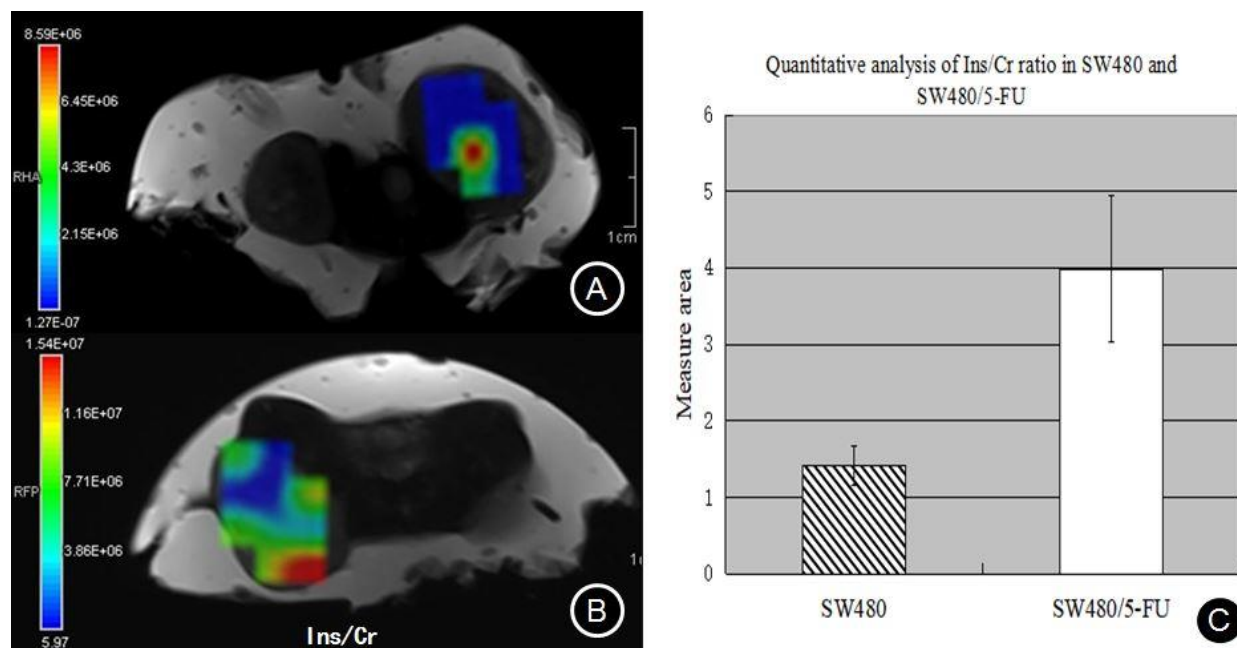


**Figure 3.** Metabolite image of the Ins/Cr profile in (A) SW480; (B) SW480/5-FU tumor tissues; (C) the area under the peak.

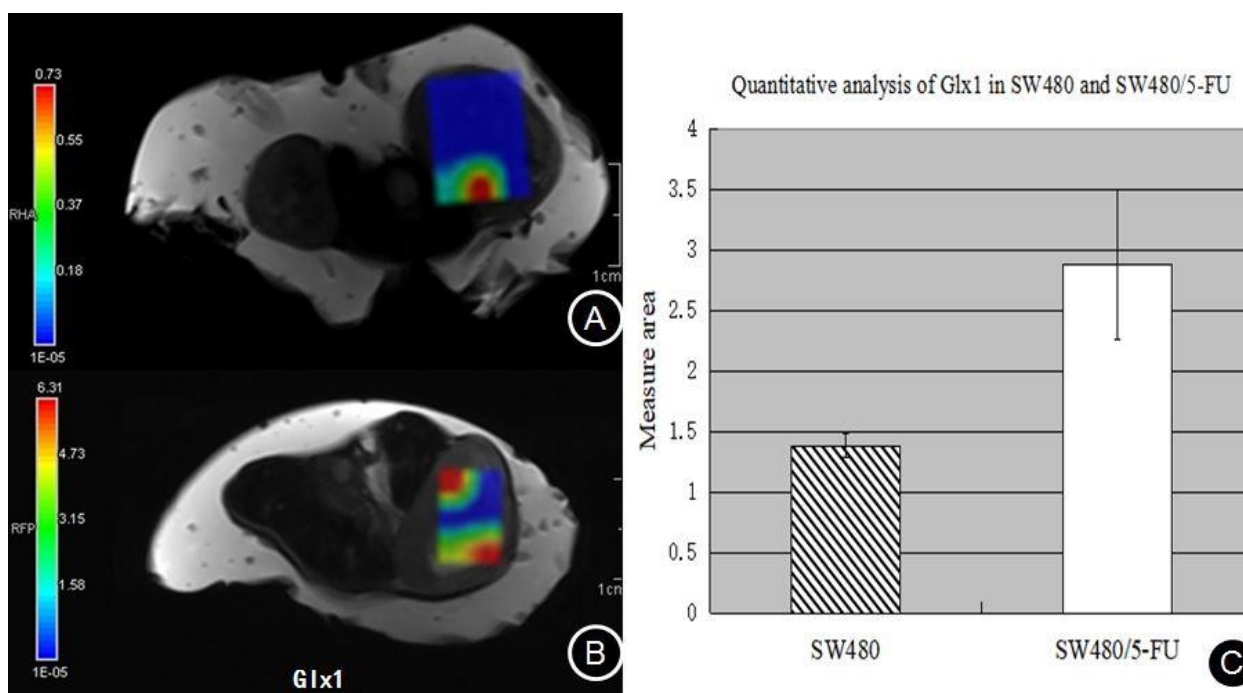


**Figure 4.** Metabolite image of the Glx1 profile in (A) SW480 ; (B) SW480/5-FU tumor tissues; (C) the area under the peak.

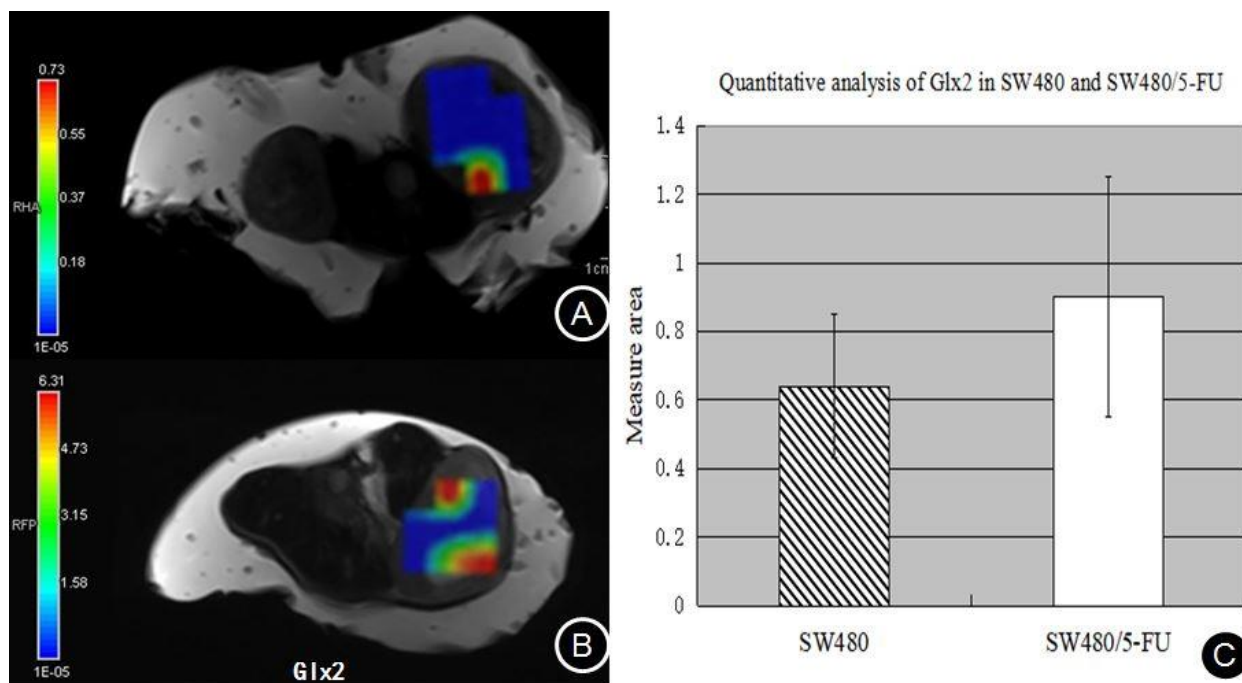


**Figure 5.** Metabolite image of the Glx2 profile in (A) SW480; (B) SW480/5-FU tumor tissues; (C) the area under the peak.

The areas under the peaks of the metabolites stated above, as well as the ratios of Ins/Cr, Glx1/Cr and Glx2/Cr, were obtained. The values of tCho, Lac, Glx1, Glx2 and Ins/Cr were significantly lower in SW480 tissues than in SW480/5-FU tissues ( $P < 0.05$ , **Table 1**).

**Table 1.** Quantitative analysis with 1H-MRS in SW480 and SW480/5-FU tumor ( $\bar{x} \pm s$ ).

Groups ( $n = 8$ )	Cho	Ins/Cr	Lac	Glx1	Glx2
SW480	$0.94 \pm 0.47$	$1.42 \pm 0.26$	$0.60 \pm 0.14$	$1.38 \pm 0.10$	$0.64 \pm 0.21$
SW480/5-FU	$2.89 \pm 0.92$	$3.99 \pm 0.96$	$1.92 \pm 0.29$	$2.88 \pm 0.62$	$1.096 \pm 0.35$
$Z/t$	2.611	2.611	9.10	-4.119	-2.469
$P$	0.008	0.008	<0.000	0.015	0.039

$Z$  and  $p$ -values are  $U$  test results of Cho and Ins/Cr between the SW480 and SW480/5-FU groups.  $t$  and  $p$ -values are  $T$ -test results of Lac and Glx (Glx1, Glx2) between the two groups.

## 3.2. Experimental evaluation of specimens

### 3.2.1. Histopathology

The degree of necrosis in tumor tissues between SW480 and SW480/5-FU on HE slices was not significantly different (**Figure 6**,  $P = 0.700$ ,  $Z = -0.471$ ). The nuclei of SW480 cells were smaller than those of SW480/5-FU cells. Compared with SW480 cells, SW480/5-FU cells arranged more closely, and the cell density was larger with a smaller cell gap (**Figure 6**).

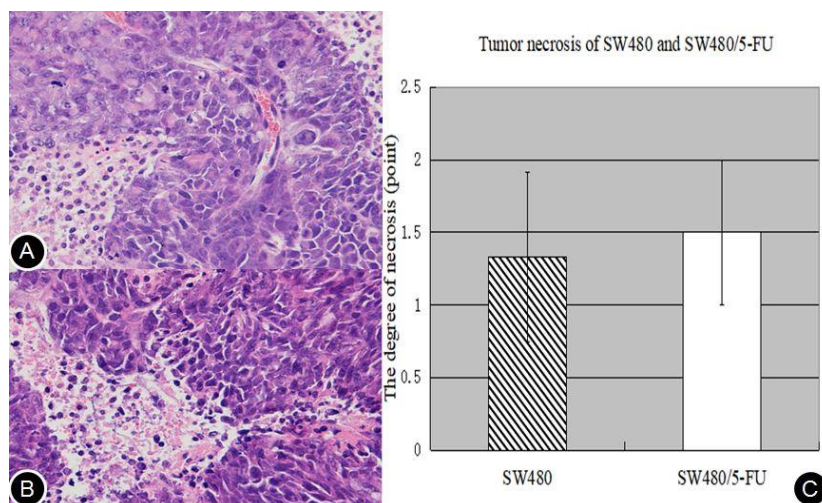


**Figure 6.** HE sections of SW480 (A, 400×)- and SW480/5-FU (B, 400×)-derived tumor tissues and (C) the degree of necrosis.

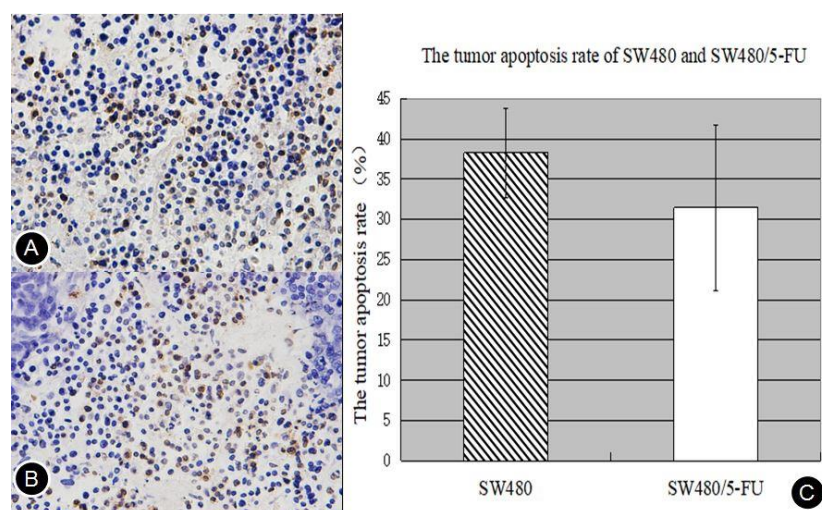


**Figure 7.** Apoptotic cells with brown staining in the nucleus scattered in (A) SW480 and (B) SW480/5-FU tumor tissues (TUNEL, 400×); (C) the apoptosis rate of tumor cells in the two groups.

Apoptotic cells with brown staining in the nucleus were observed in both SW480/5-FU and SW480 tissues (Figure 7). The apoptosis rates of tumor cells in SW480/5-FU and SW480 tissues were  $38.24 \pm 5.58\%$  and  $31.42 \pm 10.31\%$ , respectively, with no statistically significant difference ( $P = 0.400$ ;  $Z = -1.091$ ).

### 3.2.2. In vitro susceptibility test for detection of drug resistance in SW480 and SW480/5-FU xenograft tissues

According to the MTT assay, the IC<sub>50</sub> values for 5-FU in SW480/5-FU and SW480 xenograft tumor cells were  $42.9 \mu\text{g/mL}$  and  $9.516 \mu\text{g/mL}$ , respectively. The RI of SW480/5-FU xenograft tumor cells was calculated as follows:  $\text{IC}_{50} \text{ of SW480/5-FU} / \text{IC}_{50} \text{ of SW480} = 42.9 \mu\text{g/mL} / 9.516 \mu\text{g/mL} = 4.508$ . The survival rate of both groups decreased with 5-FU treatment in a concentration-dependent manner. When the concentration of 5-FU was greater than  $2.5 \mu\text{g/mL}$ , the survival rate of tumor cells in SW480 xenografts was significantly lower than that in SW480/5-FU ( $P = 0.029$ ,  $Z$

= -2.309).

### 3.2.3. Expression of proteins in tumor tissue of SW480/5-FU and SW480 xenografts

The expression of P-gp, MRP1 and PKC in tumor tissues from SW480/5-FU xenografts was increased compared with that in SW480 xenografts (**Figure 8**). There was a significant difference in the RIOD values of these protein expressions between the two groups ( $P < 0.01$ ,  $U$  test).

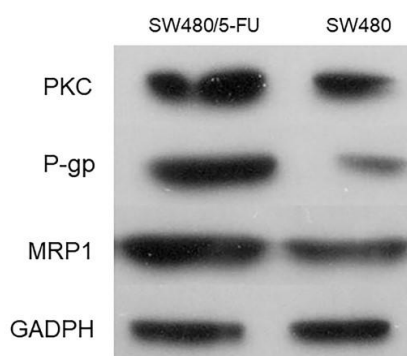


**Figure 8.** The expression of resistance-related proteins in SW480 and SW480/5-FU xenograft tumor tissues as detected by Western blotting.

### 3.3. Correlation between metabolite levels in tumor tissue detected by <sup>1</sup>H-MRS and Western blotting (Spearman correlation test)

The area of the tCho peak in the tumor had a positive correlation with the expression of P-gp ( $r$ ,  $P$ : 0.636, 0.048) and MRP1 ( $r$ ,  $P$ : 0.821, 0.004).

The area of the Lac peak in the tumor had a positive correlation with the expression of P-gp ( $r$ ,  $P$ : 0.806, 0.005).

The Ins/Cr peak area ratio had a positive correlation with the expression of P-gp ( $r$ ,  $P$ : 0.770, 0.009) and PKC ( $r$ ,  $P$ : 0.762, 0.010).

The areas of the Glx1 and Glx2 peaks in tumors had a positive correlation with the expression of MRP1 ( $r$ ,  $P$ : 0.880, 0.021; 0.847, 0.002).

## 4. Discussion

In this study, the necrosis and apoptosis rates of colon cancer cells from SW480 and SW480/5-FU xenograft tumor tissues were similar without 5-FU administration. However, the RI of SW480/5-FU xenograft tissues was almost equal to that of cancer cells in vitro. In a hostile microenvironment with 5-FU, the survival and proliferation rates of SW480/5-FU cells were significantly higher than those of SW480 cells, which indicated resistance to 5-FU in tumor tissues of the SW480/5-FU group. In addition, the expression of P-gp, MRP1, and PKC in cancer cells of the SW480/5-FU xenograft was significantly increased compared with that in SW480 xenograft cancer cells. These results indicated that the 5-FU-resistant colon cancer mouse model used in this study was reliable.

During chemotherapy, tumor cells in the microenvironment containing anticancer drugs initiate metabolic reprogramming from the gene level (genetic mutations in cell cycle pathways of cancer cells) [15–17] to the protein level (mutations in metabolic

enzymes) [17,18], which may have an impact on the metabolism of tumor cells and the surrounding tissues [17–20]. Eventually, changes in the microenvironment may support tumor survival. Therefore, metabolic changes in tumor tissues represent the final step in the biological processes of tumors, and information on the metabolites of tumors can well reflect the biological characteristics of the tumor. In vivo detection of the metabolic profiles of tumor tissues may shed light on the complex pathophysiological process of tumor drug resistance or facilitate the exploration of new biomarkers related to tumor drug resistance.

The metabolite levels in the tumor are closely related to three major metabolic pathways: glucose, amino acid, and choline phospholipid metabolism, which are significant pathways in tumorigenesis and tumor progression [20–22].

Glucose is the main source of energy and carbon in mammalian cells. Glycolysis, or glucose breakdown, leads to final products, including ATP, pyruvate, and the reduced form of nicotinamide adenine dinucleotide (NADH) [23]. Glycolysis, the TCA cycle, and oxidative phosphorylation produce ATP and together constitute cellular respiration [23]. In cancer cells and rapidly proliferating cells, most of the pyruvate produced during glycolysis is transformed into lactic acid regardless of oxygen levels (i.e., the Warburg effect) [23].

Most chemotherapeutic drugs are weakly alkaline. Hydroxide ions in drugs can be neutralized by hydrogen ions dissociated from lactic acid, making it difficult for chemotherapeutic drugs to penetrate the cell membrane and resulting in multiple drug resistance (MDR) in tumors [24]. In addition, the mechanism of tumor acidification resistance may be related to P-gp. After prostate cancer cells were cultured in acidic medium for several hours, the P-gp activity of the cells doubled, but P-gp expression remained unchanged, suggesting that P-gp increases the transmission rate under acidic conditions [25]. Research has shown that the production of Lac increases the invasiveness of tumor cells to surrounding tissues and reduces the sensitivity to the immune response and chemotherapeutic drugs, which is beneficial for tumor survival [22].

The spectral data obtained by MRS represent all observable metabolites with their individual chemical profiles in the region of interest. The corresponding peaks have their specific characteristics and positions, which are determined by the different chemical structures of the metabolites, and the peak areas reflect the concentrations of each compound [26]. Although <sup>1</sup>H-MRS has been widely applied for differentiation and staging assessment, clinical monitoring, and the treatment of central nervous system, breast, and prostate tumors [6–9,27,28], its value in detecting tumor drug resistance has rarely been reported in English literature.

In this study, <sup>1</sup>H-MRS was used to detect changes in metabolites, including tCho, Lac, Glx, Ins, and Cr, in colon cancer tissues from SW480 (responsive) or SW480/5-FU (resistant) tumor-bearing mice. The results showed that the area of the Lac peak in SW480/5-FU tissues was significantly higher than that in SW480 tissues ( $P < 0.01$ ). The area of the Lac peak was positively correlated with the expression of P-gp. This result verifies the correlation between tumor acidification resistance and P-gp in vivo.

In addition, in human cells, amino acids such as glutamine can generate ATP by replenishing intermediate metabolites for the TCA cycle [22]. Studies have shown that glutamine can be transported into cells and hydrolyzed to glutamate and ammonium

by glutaminase (GLS or GLS2) in cancer cells and rapidly dividing normal cells [29,30]. Glutamate participates in several metabolic pathways in human cells: synthesis of proteins, conversion to ketoglutarate to join the TCA cycle, acting as a precursor to the antioxidant glutathione, or providing amino groups for non-essential amino acids (e.g., alanine, aspartate, serine, and glycine) [29,30].

Glutathione, a tripeptide consisting of glutamate, cysteine, and glycine, is a major cellular antioxidant found in virtually all cells [29–31]. It plays a role in oxidation-reduction reactions, acting as a cofactor in enzyme reactions, protecting against reactive oxygen species and potentially toxic substances, and providing storage for cysteine. It also regulates cellular life activities, including gene expression, DNA and protein synthesis, cell proliferation and apoptosis, signal transduction, cytokine production and immune response, and protein glutathionylation [29,31]. Additionally, it is speculated that high levels of glutathione can increase drug resistance by reducing the ability of the drug to damage cancer cells [29,32]. Cancer cells with lower glutathione concentrations were more sensitive to radiation therapy [32]. In addition, it was observed that the drug resistance of chemo-resistant breast cancer cells was reduced with decreased glutathione levels [33].

This study found that compared with those in SW480 xenografts, the areas of the Glx1 peak and Glx2 peak were significantly higher in SW480/5-FU xenografts ( $P < 0.05$ ). The areas of the Glx1 and Glx2 peaks were positively correlated with the expression of MRP1, which suggests that the areas of the Glx1 peak and Glx2 peak can reflect the metabolic state of glutathione related to tumor drug resistance and may become biomarkers for monitoring tumor resistance in vivo.

Cho, an organic compound responsible for many essential cell functions, serves as a precursor of phosphatidylcholine (PtdCho). PtdCho is one of the main forms of phospholipids and has the highest content in eukaryotic cell membranes [34]. The decomposition products of PtdCho include 1-acylglycerophosphocholine and glycerophosphocholine (GPC). GPC is then converted to choline, completing the choline cycle [22]. Choline-containing compounds are involved in essential cell membrane phospholipid biosynthesis and degradation [35]. The rapid growth of tumor cells requires a large amount of phospholipid products such as PtdCho. Abnormally high levels of PtdCho in Cho and Cho-containing compounds could be a metabolic marker of tumor progression [36]. <sup>1</sup>H-MRS can only detect the total choline (tCho) peak in vivo. Thus, the peak of tCho may suggest the activity of tumor cell metabolism [26].

The study indicated that the area of the tCho peak in SW480/5-FU tumor tissues was significantly higher than that in SW480 tumor tissues ( $P < 0.01$ ). Assessment of HE sections demonstrated that the cellularity density of SW480/5-FU tumor tissues was higher than that of SW480. The peak area of tCho in tumors had a positive correlation with the expression of resistance-related proteins such as P-gp and MRP1. These results showed that an increase in the level of tCho is related to higher turnover in the cell membrane and higher cell density caused by cell proliferation in tumor tissues. Thus, dynamic changes in tCho measured with <sup>1</sup>H-MRS in vivo may provide insight into the pathophysiological process of tumor drug resistance transformation.

The Cr peak mainly contains creatine and phosphocreatine. When intracellular ATP is insufficient, Cr releases the high-energy phosphate bond to accelerate ATP

synthesis. The level of Cr reflects the energy metabolism state of the cell. Since the amount of Cr is relatively stable under various pathophysiological conditions, the Cr peak is often used as a reference to evaluate changes in various other metabolites in 1H-MRS [37].

Ins is a metabolite associated with the renewal of the cell membrane and the structure of the phospholipid layer of the cell. The acceleration of cell membrane renewal in any form or the destruction of the phospholipid layer in the cell membrane can lead to an increase in the concentration of Ins [37]. Ins is often involved in the activation of PKC. PKC, as a drug-associated protein, regulates the invasiveness of tumors. Studies have shown that PKC is elevated in primary brain tumors with high malignancy or invasiveness [38]. This study found that the ratio of Ins/Cr peak area and PKC protein expression was significantly higher in tumor tissues of the SW480/5-FU than in those of the SW480 ( $P < 0.01$ ). The Ins/Cr peak area ratio had a positive correlation with the expression of P-gp and PKC in colon cancer. This suggests that Ins/Cr detected by 1H-MRS may be used as a biomarker in the detection of tumor resistance in vivo.

This study is a preliminary exploration of the detection of tumor drug resistance with 1H-MRS in vivo, and there are several limitations. With a small sample size ( $n = 8$  per group), the research results have statistical bias and cannot fully represent the true characteristics of drug resistance of colon cancer. Therefore, further larger sample sizes are needed to validate the experimental results. Although customized small animal coils were used in this study, the resolution and signal-to-noise ratio of the 1H-MRS spectral data collected by clinical medical MR imaging instruments for small animals were still inferior to those collected by small animal-specific MR imaging instruments. Therefore, the reliability of metabolite detection results in this study still needs further observation and correction through the study with small animal-specific MR imaging devices. The Lac and Lip peaks overlap at 1.3 ppm of the spectrum curve collected by the PRESS of the short TE (40 ms). It is necessary to change the TE (144 ms or 30 ms) for spectrum acquisition in future research to accurately isolate the Lac peak from the Lip peak, which may increase the reliability of evaluating the changes of Lac and Lip in the formation of resistance in colon cancer. The practicality and value of 1H-MRS in the in vivo detection of metabolites also require further exploration [6].

## 5. Conclusion

Our results suggest that dynamic changes in tCho, Lac, Glx1, Glx2, and Ins/Cr detected by 1H-MRS may be used to quantify the pathophysiological processes of tumor drug resistance transformation in vivo. These metabolites may be biomarkers, and increases in their levels may be used for monitoring tumor resistance to chemotherapy drugs.

**Author contributions:** Conceptualization, QX; methodology, XYS, YMY and MYW; formal analysis, YMY, XYS and JZ; investigation, YMY, XYS and JZ; writing—original draft preparation, QX, YMY and MYW; writing—review and editing, XQ; funding acquisition, QX. All authors have read and agreed to the

published version of the manuscript.

**Funding:** This work was supported by the Natural Science Foundation of Guangdong (Grant No. 2015A030313732).

**Acknowledgments:** All authors would like to acknowledge to Gui-qin Wang (Statistician, Medical Record Management Department in Nansha, Guangzhou First People's Hospital, School of Medicine, SCUT.) for her assistance in statistical analysis.

**Institutional review board statement:** The animal study protocol was approved by the Ethical Committee of Guangzhou Medical University for Animal Research and complied with the Guide for the Care and Use of Laboratory Animals (GY2017-007, November 9th, 2017).

**Informed consent statement:** Not applicable.

**Conflict of interest:** The authors declare no conflict of interest.

## References

1. Hussen BM, Abdullah SR, Mohammed AA, et al. Advanced strategies of targeting circular RNAs as therapeutic approaches in colorectal cancer drug resistance. *Pathology - Research and Practice*. 2024; 260: 155402. doi: 10.1016/j.prp.2024.155402
2. Urso L, Uccelli L, Boschi A, et al. Molecular Imaging in Cancer Chemoresistance: What's Brewing? *Journal of Nuclear Medicine*. 2025; 66(3): 344-348. doi: 10.2967/jnumed.124.268967
3. Mourelatos D. Sister chromatid exchange assay as a predictor of tumor chemoresponse. *Mutation Research/Genetic Toxicology and Environmental Mutagenesis*. 2016; 803-804: 1-12. doi: 10.1016/j.mrgentox.2016.03.011
4. Chen Y, Chen Z, Su Y, et al. Metabolic characteristics revealing cell differentiation of nasopharyngeal carcinoma by combining NMR spectroscopy with Raman spectroscopy. *Cancer Cell International*. 2019; 19(1). doi: 10.1186/s12935-019-0759-4
5. Ma FH, Li YA, Liu J, et al. Role of proton MR spectroscopy in the differentiation of borderline from malignant epithelial ovarian tumors: A preliminary study. *Journal of Magnetic Resonance Imaging*. 2018; 49(6): 1684-1693. doi: 10.1002/jmri.26541
6. Daimiel Naranjo I, Bhowmik A, Basukala D, et al. Assessment of Hypoxia in Breast Cancer: Emerging Functional MR Imaging and Spectroscopy Techniques and Clinical Applications. *Journal of Magnetic Resonance Imaging*. 2024; 61(1): 83-96. doi: 10.1002/jmri.29424
7. Sharma U, Jagannathan NR. Magnetic Resonance Imaging (MRI) and MR Spectroscopic Methods in Understanding Breast Cancer Biology and Metabolism. *Metabolites*. 2022; 12(4): 295. doi: 10.3390/metabo12040295
8. Chawla S, Bukhari S, Afridi OM, et al. Metabolic and physiologic magnetic resonance imaging in distinguishing true progression from pseudoprogression in patients with glioblastoma. *NMR in Biomedicine*. 2022; 35(7). doi: 10.1002/nbm.4719
9. Wang L, Chen G, Dai K. [Retracted] Hydrogen Proton Magnetic Resonance Spectroscopy (MRS) in Differential Diagnosis of Intracranial Tumors: A Systematic Review. *Contrast Media & Molecular Imaging*. 2022; 2022(1). doi: 10.1155/2022/7242192
10. Yang YM. In vivo detection of the drug resistance of human colon cancer in mice with intravoxel incoherent motion diffusion imaging and proton magnetic resonance spectrum [Master thesis]. Guangzhou Medical University; 2017.
11. Xie Q, Yang YM, Wu MY, et al. Revealing Colon Cancer Resistance with Identification of Glutamate Metabolites by Proton MR Spectroscopy In Vivo and the Molecular Mechanism. *Advances in Diagnosis and Therapy of Colorectal Carcinoma*. 2024. doi: 10.5772/intechopen.1004157
12. Xie Q, Wu MY, Zhang DX, et al. Synergistic anticancer effect of exogenous wild-type p53 gene combined with 5-FU in human colon cancer resistant to 5-FU in vivo. *World Journal of Gastroenterology*. 2016; 22(32): 7342. doi: 10.3748/wjg.v22.i32.7342

13. Xie Q, Yang YM, Wang GQ, et al. Preliminary Study on Monitoring Drug Resistance of Colon Cancer with Intravoxel Incoherent Motion MRI in Vivo. *J Clin Med Img.* 2023; V7(6): 1-8.
14. Workman P, Aboagye EO, et al. Guidelines for the welfare and use of animals in cancer research. *British Journal of Cancer.* 2010; 102(11): 1555-1577. doi: 10.1038/sj.bjc.6605642
15. Otto AM. Warburg effect(s)—a biographical sketch of Otto Warburg and his impacts on tumor metabolism. *Cancer & Metabolism.* 2016; 4(1). doi: 10.1186/s40170-016-0145-9
16. Wolpaw AJ, Dang CV. MYC-induced metabolic stress and tumorigenesis. *Biochimica et Biophysica Acta (BBA) - Reviews on Cancer.* 2018; 1870(1): 43-50. doi: 10.1016/j.bbcan.2018.05.003
17. Li G, Che X, Wang S, et al. The role of cisplatin in modulating the tumor immune microenvironment and its combination therapy strategies: a new approach to enhance anti-tumor efficacy. *Annals of Medicine.* 2025; 57(1). doi: 10.1080/07853890.2024.2447403
18. Srinivasan R, Ricketts CJ, Sourbier C, et al. New Strategies in Renal Cell Carcinoma: Targeting the Genetic and Metabolic Basis of Disease. *Clinical Cancer Research.* 2015; 21(1): 10-17. doi: 10.1158/1078-0432.ccr-13-2993
19. Chen Y, Zhang Z, Ji K, et al. Role of microplastics in the tumor microenvironment (Review). *Oncology Letters.* 2025; 29(4): 1-14. doi: 10.3892/ol.2025.14939
20. Haukaas T, Euceda L, Giskeødegård G, et al. Metabolic Portraits of Breast Cancer by HR MAS MR Spectroscopy of Intact Tissue Samples. *Metabolites.* 2017; 7(2): 18. doi: 10.3390/metabo7020018
21. Huang S, Shi J, Shen J, et al. Metabolic reprogramming of neutrophils in the tumor microenvironment: Emerging therapeutic targets. *Cancer Letters.* 2025; 612: 217466. doi: 10.1016/j.canlet.2025.217466
22. Brahim-Horn MC, Bellot G, Pouysségur J. Hypoxia and energetic tumour metabolism. *Current Opinion in Genetics & Development.* 2011; 21(1): 67-72. doi: 10.1016/j.gde.2010.10.006
23. Vander Heiden MG, Cantley LC, Thompson CB. Understanding the Warburg Effect: The Metabolic Requirements of Cell Proliferation. *Science.* 2009; 324(5930): 1029-1033. doi: 10.1126/science.1160809
24. Li RT, Qian XP, Liu BR. The pH-induced physiological drug resistance and the strategies in the treatment of malignant tumors. *Tumor.* 2012; 032(005): 384-388. doi: 10.3781/j.issn.1000-7431.2012.05.014
25. Thews O, Gassner B, Kelleher DK, et al. Impact of Extracellular Acidity on the Activity of P-glycoprotein and the Cytotoxicity of Chemotherapeutic Drugs. *Neoplasia.* 2006; 8(2): 143-152. doi: 10.1593/neo.05697
26. Fardanesh R, Marino MA, Avendano D, et al. Proton MR spectroscopy in the breast: Technical innovations and clinical applications. *Journal of Magnetic Resonance Imaging.* 2019; 50(4): 1033-1046. doi: 10.1002/jmri.26700
27. Bulik M, Jancalek R, Vanicek J, et al. Potential of MR spectroscopy for assessment of glioma grading. *Clinical Neurology and Neurosurgery.* 2013; 115(2): 146-153. doi: 10.1016/j.clineuro.2012.11.002
28. Kobus T, van der Laak JAWM, Maas MC, et al. Contribution of Histopathologic Tissue Composition to Quantitative MR Spectroscopy and Diffusion-weighted Imaging of the Prostate. *Radiology.* 2016; 278(3): 801-811. doi: 10.1148/radiol.2015142889
29. Dong C, Zhao Y, Han Y, et al. Targeting glutamine metabolism crosstalk with tumor immune response. *Biochimica et Biophysica Acta (BBA) - Reviews on Cancer.* 2025; 1880(1): 189257. doi: 10.1016/j.bbcan.2024.189257
30. Bin Wan Mohd Nor WMFS, Kwong SC, Fuzi AAM, et al. Linking microRNA to metabolic reprogramming and gut microbiota in the pathogenesis of colorectal cancer (Review). *International Journal of Molecular Medicine.* 2025; 55(3). doi: 10.3892/ijmm.2025.5487
31. Rae CD, Williams SR. Glutathione in the human brain: Review of its roles and measurement by magnetic resonance spectroscopy. *Analytical Biochemistry.* 2017; 529: 127-143. doi: 10.1016/j.ab.2016.12.022
32. Traverso N, Ricciarelli R, Nitti M, et al. Role of Glutathione in Cancer Progression and Chemoresistance. *Oxidative Medicine and Cellular Longevity.* 2013; 2013: 1-10. doi: 10.1155/2013/972913
33. Cioce M, Valerio M, Casadei L, et al. Metformin-induced metabolic reprogramming of chemoresistant ALDHbright breast cancer cells. *Oncotarget.* 2014; 5(12): 4129-4143. doi: 10.18632/oncotarget.1864
34. Gibellini F, Smith TK. The Kennedy pathway—De novo synthesis of phosphatidylethanolamine and phosphatidylcholine. *IUBMB Life.* 2010; 62(6): 414-428. doi: 10.1002/iub.337
35. Tayari N, Heerschap A, Scheenen TWJ, et al. In vivo MR spectroscopic imaging of the prostate, from application to interpretation. *Analytical Biochemistry.* 2017; 529: 158-170. doi: 10.1016/j.ab.2017.02.001
36. Glunde K, Bhujwalla ZM, Ronen SM. Choline metabolism in malignant transformation. *Nature Reviews Cancer.* 2011;

11(12): 835-848. doi: 10.1038/nrc3162

37. Shah N, Sattar A, Benanti M, et al. Magnetic resonance spectroscopy as an imaging tool for cancer: a review of the literature. *J Am Osteopath Assoc.* 2006; 106(1): 23-27.
38. McCoy ES, Haas BR, Sontheimer H. Water permeability through aquaporin-4 is regulated by protein kinase C and becomes rate-limiting for glioma invasion. *Neuroscience.* 2010; 168(4): 971-981. doi: 10.1016/j.neuroscience.2009.09.020